A Physics-based and Control-oriented Model for Dielectric Elastomer Tubular Actuator

Theophilus Kaaya, Shengbin Wang, Marzia Cescon, Zheng Chen*

Abstract—Dielectric elastomers (DEs) are electro-active polymers that deform and change their shape when an electric field is applied across them. They are used as soft actuators since they are flexible, resilient, lightweight, and durable. Many models have been proposed to describe and capture the behavior of these actuators such as circuit representation, lumped parameter modeling, and physics-based modeling. In this paper, a hybrid between the physics and lumped parameter model is presented which is used to control the actuator. The focus of this paper is on a tubular dielectric elastomer actuator (DEA). The model proposed is validated with experimental data to evaluate its approximation to the physical actuator. The physics model offers the ability to describe how the material properties and actuator's geometry affect the dynamics and behavior of the actuator under different states. The lumped parameter model accounts for physical quantities that may not be fully expressed when formulating the physics-based equations. The discussed model performance is found to have an error less than 10% for the sinusoidal signals discussed.

Keywords— Dielectric elastomer actuator, Tubular actuator, Finite Element

I. INTRODUCTION

Dielectric elastomer actuators (DEAs), a class of electro active polymers, offer promising properties over conventional actuators in that they are compact and do not require a large amount of space to operate [1]. They are flexible and as such can be molded to take up different shapes yet still offer optimal performance. They are also quiet hence reduce noise pollution under operation compared to conventional rigid actuators. Due to their low noise production, DEAs can be employed in research areas such as marine and aquatic research to effectively study fish and marine life with minimal interference [2]. In their simplest configuration, they are easy to manufacture and the material is readily available [3]. The actuators are light weight which means that they can be carried easily such as on an individual's body, in generators, and loud speakers [4]. In addition, they offer large amounts of strain when a voltage is applied across the membranes of the actuators. They have a high elastic energy density that can be harnessed to produce large deformations and electric generation [5]. The DEAs are also called artificial muscles used to mimic the movement of muscles in the design of bionic robots and in prosthesis to help disabled people recover their movement and function

of lost limbs [6]. The DEA's performance and characteristics render them ideal in soft robotics. Current work on dielectric tubular actuators has found its application in refreshable braille displays [7], push actuators [8], and active vibration isolation [9] to mention but a few.

With all these benefits however, the dielectric actuators are challenging to model and their behavior is unpredictable in certain configurations [10]. To achieve all the benefits that DEAs offer, research has been conducted to study and model the dielectric elastomers. Circuit based models have been devised along with frequency based models that capture the actuator's dynamics [11], [12] to analyze the dynamics of the actuators. These methods ignore the actual physics of the actuators and as such do not explain in effect the coupling between the mechanical and electrical quantities of the actuator as well as its geometry. The control of these actuators is also still challenging and is an area of open research [13]. Research is also focused on developing fundamental models from which more complex models can be developed to advance the development of dielectric actuators [14]. Current physics model based work depends on static based analysis of the actuators. In this paper the quasi static model is extended into a dynamic model do analyze the dynamics of the actuator.

Different configurations exist for dielectric actuators such as stacked, diaphragm, rolled, and tubular. Stacked and rolled configurations offer the ability for increased displacement and force generated by the actuator. The diaphragm can be made as thin as possible but occupies space in the transverse direction. The tubular actuator combines the advantage of the stacked and diaphragm actuator to allow space conservation while still maintain a reasonable amount of displacement and force that can be produced by the actuator. A physics-lumped parameter based model of the tubular dielectric actuator which can be used to predict the behavior of the DEA is presented in this paper. The derivation process follows closely that of Tianhu He *et al.* [15] with modifications specific to the tubular dielectric actuator.

Since the actuator is a physical system, the governing equations must produce positive stretch values for the actuator. The major contribution of this paper is the introduction of a methodology in solving the differential equations that arise from the physics of the actuator to guarantee positive stretch values while solving the differential equations. As will be seen in the following discussion, the longitudinal stretch of the actuator is solved from a quadratic algebraic equation which poses a challenge of having multiple solutions to the stretch. Instead of solving the roots of the algebraic equation

^{*}Corresponding author: Zheng Chen, Email: zchen43@central.uh.edu. This work was supported in part by the National Science Foundation under Grant CMMI #1747855.

T. Kaaya, S. Wang, M. Cescon, and Z. Chen are with the University of Houston, Mech. Eng. Dept, 4800 Calhoun Rd, Houston TX 77004. tskaaya@uh.edu, swang62@uh.edu, mcescon2@uh.edu, zchen43@central.uh.edu

each time, the equation is transformed into a differential equation to track the locus of the positive stretch value of the actuator. The advantage is that instead of solving three ordinary differential equations (ODEs) with a constraint, the numerical problem simply becomes one of solving four ODEs without constraint. Lastly, this also ensures that we arrive at one unique solution for the tubular actuator given the fact that the shooting method, which may potentially produce multiple solutions, is used to arrive at the desired solution. Secondly, since the equations derived are quasistatic, a case of a fictitious damping coefficient is introduced into the system by taking the derivative of the algebraic equation with velocity to account for the viscoelasticity of the actuator.

The rest of the paper is organized as follows: Section II presents a quasi-static nonlinear electromechanical model of the DEA. Section III covers the state space model of the DEA, Section IV discusses the numerical simulation for the tubular actuator. Section V provides the experimental setup and validation of the tubular actuator model. Section VI discusses the conclusions and future work.

II. MODELING OF THE DIELECTRIC ELASTOMER (DE) TUBULAR ACTUATOR

In this section, the governing equations that describe the shape and behaviour of the tubular actuator are derived. Figure 1 shows a cross section of the tubular actuator in the undeformed state (a) and deformed state (b).

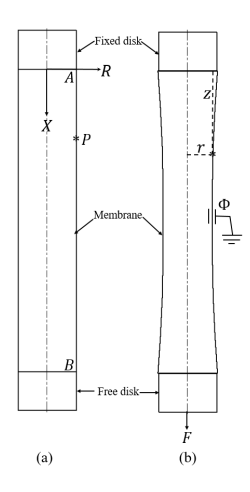


Fig. 1. Cross section of tubular actuator in undeformed state (a), and deformed state (b).

In the current configuration, the actuator is fixed at the top and free to move at the bottom. The actuator is given a pre-stretch in the longitudinal direction (X-axis) by attaching a weight at the bottom. The attached weight has significant effects on the behavior of the actuator since it shifts the actuator from one mode (state) to another.

Considering specific points (particles) on the membrane at A and B. The particles at A are constrained by the fixed top disk and do not move during actuation while those at B are free to move vertically but are constrained by the bottom

disk to disk radius R. All other points on the membrane are located at the radius R and depth X forming the reference coordinate system (X,R) where R is fixed in the undeformed state. A general particle p at (X,R) in the undeformed state moves to a location (r,z) in the current coordinate system (deformed state) when a vertical force F, or an applied voltage Φ , or both are exerted onto the membrane.

Take an element on the actuator with one end at (X,R) and another at (X+dX,R) where dX is the elemental length in the undeformed state. These ends undergo deformation to occupy the new locations (r(X),z(X)) and (r(X+dX),z(X+dX)) respectively. Let the particles in the deformed state be separated by a distance dl forming an angle θ with the horizontal measured from the second point counterclockwise. The change in r and in z is given by dr = r(X+dX) - r(X) and dz = z(X+dX) - z(X). Since the orientation of the element changes with X, then

$$dr = -dl\cos(\theta)$$
 $dz = dl\sin(\theta)$. (1)

For this element, $dl^2 = dr^2 + dz^2$. The geometry of the actuator is thus fully described.

To characterize the mechanical and electrical components of the actuator, three parameters are defined: The longitudinal stretch (along the X-axis), λ_1 , and latitudinal (circumferential) stretch, λ_2 ,

$$\lambda_1 = \frac{dl}{dX} = \sqrt{(\frac{dr}{dX})^2 + (\frac{dz}{dX})^2}, \quad \lambda_2 = \frac{2\pi r}{2\pi R} = \frac{r}{R},$$
 (2)

and the nominal charge density, $\bar{D}=\frac{q}{A_0}$ where q is the charge on the element and A_0 is the elemental area in the undeformed state. These three parameters $\lambda_1,\,\lambda_2,\,$ and \bar{D} fully describe the deformation of the actuator to an applied load F and/or voltage Φ . The total charge Q on the actuator is given as $Q=2\pi R\int \bar{D}dX$.

Since the actuator relies on the ability of the dielectric membrane to undergo large strain deformations, Helmholtz's energy, $E_H = 2\pi R H \int W dX$ is used do describe the energy of the actuator. W is the nominal Helmholtz's energy assumed to be a function of λ_1 , λ_2 , and \bar{D} and H the thickness of the membrane in the undeformed state. For a small change in λ_1 , λ_2 , and \bar{D} , the Helmholtz's energy undergoes a change $\delta W = s_1 \delta \lambda_1 + s_2 \delta \lambda_2 + \bar{E} \delta \bar{D}$, where

$$s_1 = \frac{\partial W}{\partial \lambda_1}, \qquad s_2 = \frac{\partial W}{\partial \lambda_2}, \qquad \bar{E} = \frac{\partial W}{\partial \bar{D}}.$$
 (3)

 s_1 , s_2 , and \bar{E} are the longitudinal nominal stress, the circumferential nominal stress, and the nominal electric field respectively.

In a state of equilibrium, the change in the Helmholtz's energy of the actuator is equal to the work done in moving the actuator from one state to another through the work done by the applied force and voltage. Therefore

$$\delta E_H = 2\pi R H \int \delta W dX = F \delta z_B + \Phi \delta Q,$$
 (4)

also

$$\int \delta W dX = \int (s_1 \delta \lambda_1 + s_2 \delta \lambda_2 + \bar{E} \delta \bar{D}) dX, \qquad (5)$$

where

$$\delta \lambda_1 = -\cos(\theta) \frac{d(\delta r)}{dX} + \sin(\theta) \frac{d(\delta z)}{dX}, \tag{6}$$

$$\delta \lambda_2 = \frac{\delta r}{R} \qquad \qquad \delta \bar{D} = \frac{\delta Q}{A_0}. \tag{7}$$

To this end, solving Eq. 5 over the entire length of the actuator from A to B and substituting into Eq. 4 gives

$$\frac{d(s_1\cos\theta)}{dX} = -\frac{s_2}{R}, \quad 2\pi R H s_1 \sin\theta = F, \quad H\bar{E} = \Phi. \quad (8)$$

Eq. 8 describes the equations of state of the actuator.

For the material model of the actuator, the actuator is assumed to be an ideal in-compressible dielectric elastomer. In assuming in-compressibility, the stretch in the thickness direction is given by λ_3 =1/ $\lambda_1\lambda_2$. For the ideal actuator, the dielectric property of the actuator is not affected by deformation hence the dielectric constant, ε_r is assumed to be fixed. For simplicity, a neo-hookean model is chosen to characterize the actuator's free-energy density. Other models such as the Yeoh model, and the Ogden model may be employed to get more accurate results that cover larger strains in the actuator [16]. The neo-hookean model is given by

$$W(\lambda_1, \lambda_2, \bar{D}) = \frac{\mu}{2} (\lambda_1^2 + \lambda_2^2 + \lambda_1^{-2} \lambda_2^{-2} - 3) + \frac{\bar{D}^2}{2\varepsilon} \lambda_1^{-2} \lambda_2^{-2},$$

where μ is the shear modulus of the actuator and ε the permittivity of the membrane. From Eq. 9, Eq. 3 is solved to obtain

$$s_1 = \mu(\lambda_1 - \lambda_1^{-3}\lambda_2^{-2}) - \frac{\bar{D}^2}{\varepsilon}\lambda_1^{-3}\lambda_2^{-2},$$
 (9)

$$s_2 = \mu(\lambda_2 - \lambda_2^{-3}\lambda_1^{-2}) - \frac{\bar{D}^2}{\varepsilon}\lambda_2^{-3}\lambda_1^{-2},$$
 (10)

$$\bar{E} = \frac{\bar{D}}{\varepsilon} \lambda_1^{-2} \lambda_2^{-2}. \tag{11}$$

To investigate this model, the differential equations that characterize the shape of the actuator as well as the mechanical and electrical properties of the actuator are normalized as follows: The applied load as $F^*=F/2\pi H\mu$, the applied voltage $\Phi^*=\Phi/(H\sqrt{\mu/\epsilon})$, the vertical deformed position $z^*=z/L$, and the radial deformation $r^*=r/R$.

Eq. 1 and Eq. 2 give

$$\frac{dr}{dX} = -\lambda_1 \cos \theta, \qquad \frac{dz}{dX} = \lambda_1 \sin \theta. \tag{12}$$

Differentiating the second equation in Eq. 8 with respect to X and combining it with the first equation in Eq. 8 gives

$$\frac{d\theta}{dX} = \frac{s_2}{s_1 R} \sin \theta. \tag{13}$$

Finally the algebraic equation from $2\pi R H s_1 \sin \theta = F$ can be written as

$$\left[1 - \left(\frac{\Phi^* r}{R}\right)^2\right] \lambda_1^4 - \frac{F^*}{R\sin(\theta)} \lambda_1^3 - \left(\frac{R}{r}\right)^2 = 0.$$
 (14)

Eq. 12–14 form the governing equations of the tubular actuator.

III. STATE SPACE MODEL OF DE TUBULAR ACTUATOR

A dynamic model is developed from the quasi-static model established in section II using the theory of elasticity and electrostatics and combining with Newton's second law of motion. To account for viscous effects, lumped parameter damping is introduced into the force balance of the actuator. The acceleration of the actuator is given by

$$a^* = g^* - \frac{R\sin(\theta)}{m\lambda_1^3} \left(\left\lceil 1 - \left(\frac{\Phi^* r}{R}\right)^2 \right\rceil \lambda_1^4 - \left(\frac{R}{r}\right)^2 \right) - \frac{c^*}{m} v$$

where $a^* = a/2\pi H\mu$ is the normalized acceleration, $g^* = g/2\pi H\mu$ the normalized gravity, $c^* = c/2\pi H\mu$ the normalized damping coefficient, and v the velocity of the actuator. Taking the total stretch as $\lambda_i = \lambda_i^a \lambda_i^p$ with λ_i^a as the stretch due to actuation, λ_i^p the pre-strech due to the added weight, and i = 1, 2, 3, the acceleration can be written as

$$\begin{split} a^* &= \frac{R \sin \theta}{m (\lambda_1^p)^3} \left\{ (1 - \lambda_1^a) (\lambda_1^p)^4 + \left(\frac{1}{(\lambda_2^a)^2 (\lambda_1^a)^3} - 1 \right) \frac{1}{(\lambda_2^p)^2} \right. \\ &\left. + \left(\Phi^* r \lambda_2^a \lambda_2^p \right)^2 \lambda_1^a (\lambda_1^p)^4 \right\} - \frac{c^*}{m} v \end{split}$$

Assuming small prestretch, $\lambda_i^p \approx 1$, the acceleration may be rewritten to include only the actuated stretch terms

$$a^* = -\frac{R\sin(\theta)}{m\lambda_1^3} \left(\left[1 - \left(\frac{\Phi^* r}{R}\right)^2 \right] \lambda_1^4 - \left(\frac{R}{r}\right)^2 \right) - \frac{c^*}{m} v$$

where λ_i^a is replaced with λ_i for neatness.

Eq. 14 is rewritten to serve as the spring for the actuator. Treating the actuator as a classic RC circuit for simplification purposes, a relationship between the driving nomalized voltage, u^* , and the nomalized voltage on the membrane, Φ^* , is given by

$$\dot{\Phi}^* = -\frac{\Phi^*}{RC} + \frac{u^*}{RC},$$

where R is the circuit resistance and C is the membrane capacitance and $u^* = \frac{u}{H} \sqrt{\frac{\varepsilon}{\mu}}$.

Let x_1 be the position of the bottom disk of the actuator and $v = x_2 = \dot{x}_1$ the velocity. Then its acceleration is $a^* = \ddot{x}_1 = \dot{x}_2$. Finally let $x_3 = \Phi^*$, this gives the dynamic model of the tubular actuator as Eq. 12, 13 and

$$\begin{split} \dot{x}_1 &= x_2, \\ \dot{x}_2 &= -\frac{R\sin(\theta)}{m\lambda_1^3} \left(\left[1 - \left(\frac{x_3 r}{R} \right)^2 \right] \lambda_1^4 - \left(\frac{R}{r} \right)^2 \right) - \frac{c^*}{m} x_2, \\ \dot{x}_3 &= -\frac{x_3}{RC} + \frac{u^*}{RC}. \end{split}$$

The dynamics are evaluated at the equilibrium point where the tubular actuator settles under a constant mechanical load. It is at this point that the model is also linearized. In order to complete linearization, note that r, z, θ , and λ_1 are also functions of x_1 , x_3 , and time t. Assuming small perturbations about the equilibrium point and that the shape of the actuator does not change significantly for small actuation, the first

three differential equations may be ignored which helps to reduce the order of the system to leave behind three states (x_1, x_2, x_3) . The Jacobian, J of the system takes the form

$$\mathbf{J} = \begin{bmatrix} \frac{\partial \dot{x}_1}{\partial x_1} & \frac{\partial \dot{x}_1}{\partial x_2} & \frac{\partial \dot{x}_1}{\partial x_3} \\ \frac{\partial \dot{x}_2}{\partial x_1} & \frac{\partial \dot{x}_2}{\partial x_2} & \frac{\partial \dot{x}_2}{\partial x_3} \\ \frac{\partial \dot{x}_3}{\partial x_1} & \frac{\partial \dot{x}_3}{\partial x_2} & \frac{\partial \dot{x}_3}{\partial x_3} \end{bmatrix} = \begin{bmatrix} 0 & 1 & 0 \\ f_1 & f_2 & f_3 \\ 0 & 0 & -\frac{1}{RC} \end{bmatrix}$$

The linearized state space model is therefore

$$\begin{bmatrix} \dot{x}_1 \\ \dot{x}_2 \\ \dot{x}_3 \end{bmatrix} = \begin{bmatrix} 0 & 1 & 0 \\ f_1 & f_2 & f_3 \\ 0 & 0 & -\frac{1}{RC} \end{bmatrix} \begin{bmatrix} x_1 \\ x_2 \\ x_3 \end{bmatrix} + \begin{bmatrix} 0 \\ 0 \\ \frac{1}{RC} \end{bmatrix} u.$$
 (15)

It can be observed from the second state that the actuator acts as a spring-mass-damper system with f_1 as the spring constant and f_2 the damping ratio. For a model without viscosity, $f_2 = 0$. f_3 serves as the input gain from the voltage applied onto the membrane. Hence, \dot{x}_1 and \dot{x}_2 serve as a second order system that is driven by \dot{x}_3 a first order system for the circuit model of the tubular actuator. Furthermore an expression of the transfer function of the voltage input u to the disk position x_1 is given as

$$G(s) = \frac{\frac{f_3}{RC}}{s^3 + (\frac{1}{RC} - f_2)s^2 - (f_1 + \frac{f_2}{RC})s - \frac{f_1}{RC}}.$$
 (16)

The parameters f_1 , f_2 , f_3 , and $\frac{1}{RC}$ can now be determined with frequency response analysis by inspecting the frequency response of the actuator over the range [0.02-8] Hz and fitting a transfer function onto the data.

IV. NUMERICAL SIMULATION AND RESULTS

The algebraic equation is analyzed to establish the number of permissible stretch values of λ_1 . It is worth noting that the stretch must be a positive value at all times since this is a physical system. Let

$$A = \left[1 - \left(\frac{\Phi^* r}{R}\right)^2\right], \quad B = \frac{F^*}{R\sin(\theta)}, \quad C = \left(\frac{R}{r}\right)^2$$

such that the algebraic equation becomes

$$A\lambda_1^4 - B\lambda_1^3 - C = 0. \tag{17}$$

It can be observed that for the tubular actuator described above, B and C can never have a sign change since for B the interval for θ is (0,90]. On the other hand, A can have a sign change if $\left(\frac{\Phi^*r}{R}\right)^2 > 1$. This condition can be used to find the maximum allowable theoretical voltage that may be applied on the actuator before it breaks down. It is required that A be positive at all times. Using Routh Hurwitz stability criterion,

$$\lambda_1^4 \quad A \quad 0 \quad -C
\lambda_1^3 \quad -B \quad 0 \quad 0
\lambda_1^2 \quad \varepsilon \quad -C
\lambda_1^1 \quad \frac{-BC}{\varepsilon}
\lambda_1^0 \quad -C$$
(18)

It can be observed that the elements above and below the ε in the first column have the same sign therefore a pair of imaginary roots exists in the algebraic equation. There is also a single sign change which implies that there is always one positive root whenever A is positive. The fourth remaining root is therefore negative. From this observation the requirement for keeping A positive at all times can be justified. This observation is useful when running the numerical simulation as it is the basis used to keep track of the positive root locus of the algebraic equation when solving the differential equations. To track this root, the algebraic equation is differentiated with respect to X to end up with

$$\frac{d\lambda_1}{dX} = \frac{-\frac{F^*\cos\theta\lambda_1^3}{R\sin^2\theta} \cdot \frac{d\theta}{dX} - 2\left[\frac{R^2}{r^3} - r\left(\frac{\Phi^*}{R}\right)^2\lambda_1^4\right]\frac{dr}{dX}}{\left(4\left[1 - \left(\frac{\Phi^*r}{R}\right)^2\right]\lambda_1 - \frac{3F^*}{R\sin\theta}\right)\lambda_1^2}.$$
 (19)

The four differential equations 12-13, and 19 can now be solved numerically. Considering the boundary conditions, the actuator is a two boundary valued problem with the boundaries being r(0) = r(L) = R where L is the total length of the actuator in the undeformed state. z(0) = 0 but z(L) is unknown as well as $\theta(0)$, $\theta(L)$ and $\lambda_1(0)$. In order to establish $\lambda_1(0)$ we need to solve the algebraic equation given r(0) and $\theta(0)$. As such, the system is solved using the shooting method in which an initial guess of $\theta(0)$ that satisfies the two boundary conditions r(0) = r(L) = R is made. The parameters used in the simulation are R = 7.5 mm, H = 0.26 mm, and L = 80 mm.

The value of the shear modulus is chosen and calibrated to closely fit the experimental data collected for multiple applied loads. It should be noted that the shear modulus is a function of temperature and frequency of actuation of the actuator attributed to the viscous effect of the VHB tape [17]. The simulation is run with F = 20 g and $\Phi = 0$ V along with the following parameters: A membrane thickness of 0.25 mm, a height of 80 mm, a shear modulus of 18.5 kPa, and relative permittivity of 2.7. This particular simulation is performed using MATLAB R2019a. For a given $\theta(0)$ the positive value of $\lambda_1(0)$ is calculated by solving the roots of the algebraic equation and choosing the positive root. This value is the one that is then used to solve Eq. 19 and with this, each iteration of the numerical simulation ensures that λ_1 is always positive since the starting value of the iteration is positive. With r(0), $\theta(0)$, z(0), and $\lambda_1(0)$, the rest of the differential equations are solved using ode45 to produce r(X), z(X), $\theta(X)$, and $\lambda_1(X)$. Post processing is performed on these variables such as estimating the behavior and trend of displacement vs applied voltage and displacement vs load. Figure 2 and Fig. 3 show these trends respectively. Furthermore the model can be used to perform closed loop control.

V. EXPERIMENTAL SETUP AND MODEL VALIDATION

A. Experimental setup

The actuator is made from VHB material of 10 cm by 5.6 cm size cut from a tape roll. Both ends are fixed on

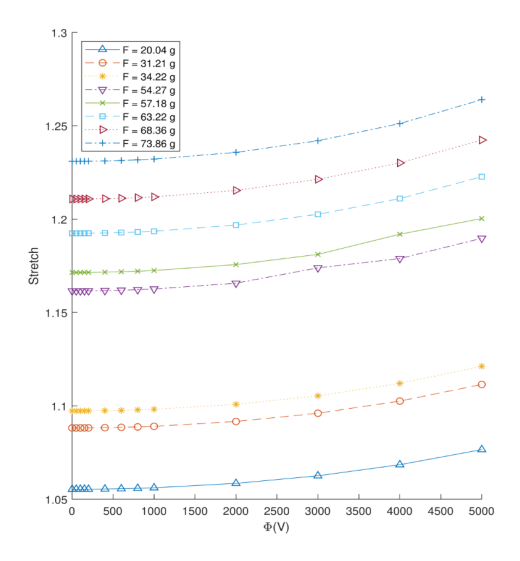


Fig. 2. Stretch vs Applied voltage

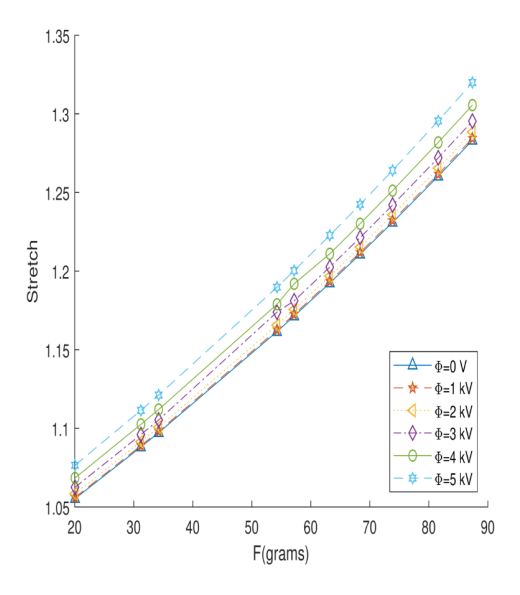


Fig. 3. Stretch vs applied load.

plastic cylinders. The edges of the sides are then covered with insulating tape to avoid short circuit between the two electrodes. Graphite powder is pasted on both sides of the DE membrane uniformly, and a load of 20 g is fixed on the lower end to contribute a vertical pre-stretch of 137.5 %. The final length of the DE tube is 110 mm. The DE tube membrane actuator and full experimental setup is shown in Fig. 4. The laser sensor measures the movement of the DE tube by measuring the displacement between the laser sensor and the wooden balance plate.

B. Model validation

A sinusoidal input signal of amplitude 2 kV is used. The output for the displacement magnitude of the DE tube is measured by the laser sensor with units in mm. A 20 g load is placed on the free end of the DE tube. The actuation voltage

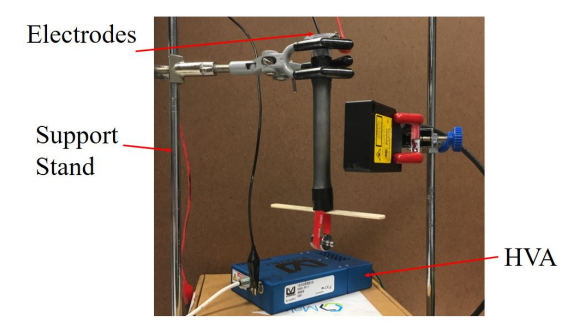


Fig. 4. Experimental setup

is provided by a high voltage amplifier (5HVA24-BP1-F). A transfer function is estimated from the experimental data from which the values of f1, f2, f3, and 1/RC can be calculated. Figure 5 shows the bode diagram of the tubular actuator.

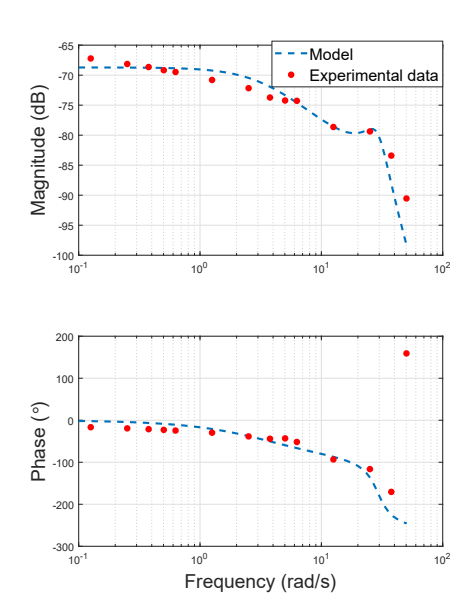


Fig. 5. Frequency response of the actuator.

The transfer function of the tubular actuator is given as:

$$G(s) = \frac{1.1}{s^3 + 16s^2 + 900s + 3000}. (20)$$

The parameters f_1 , f_2 , f_3 , and $\frac{1}{RC}$ are thus determined as $f_1 = -856.2159$, $f_2 = -12.4962$, $f_3 = 0.3139$, and $\frac{1}{RC} = 3.5038$. The time constant τ for the electric circuit is therefore 0.2854 s. The state space model is:

$$\begin{bmatrix} \dot{x}_1 \\ \dot{x}_2 \\ \dot{x}_3 \end{bmatrix} = \begin{bmatrix} 0 & 1 & 0 \\ -856.2159 & -12.4962 & 0.3139 \\ 0 & 0 & -3.5038 \end{bmatrix} \begin{bmatrix} x_1 \\ x_2 \\ x_3 \end{bmatrix} + \begin{bmatrix} 0 \\ 0 \\ 3.5038 \end{bmatrix} u. (21)$$

Reference tracking with PI control is performed using the model and compared with experimental data. Figure 6 shows the comparison between the linear model and experimental

data. The model closely predicts the displacement of the tubular DEA.

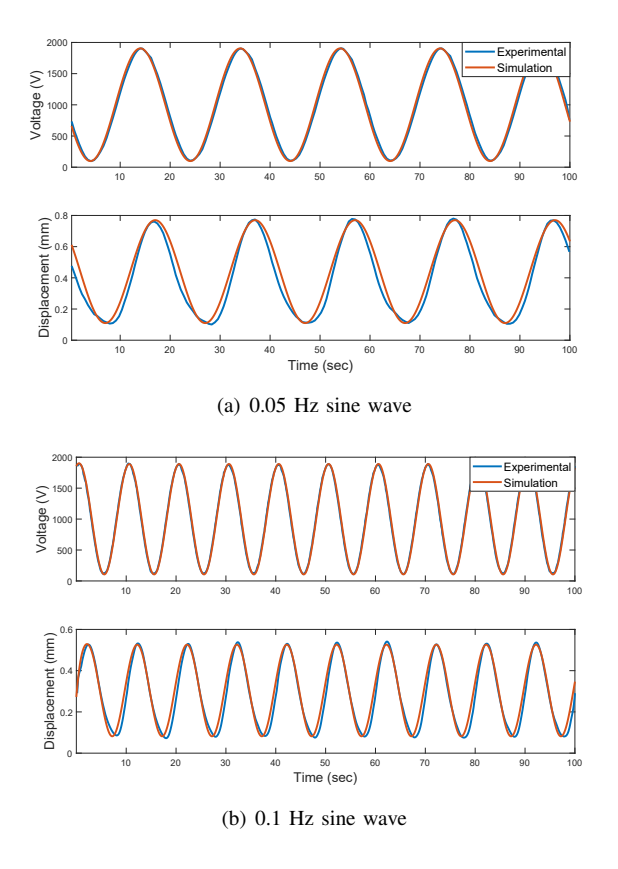


Fig. 6. (a) 0.05 Hz sinusoidal and (b) 0.1 Hz sinusoidal reference tracking.

The error between the model and the experimental data is (5.70%, 3.64%) corresponding to a 0.05 Hz, 0.1 Hz sinusoidal reference tracking. This is obtained by taking the root-mean-square value of the error between the experimental data and the simulated data. The model can fairly track and predict the actuator response even with the constraints imposed from the simplifications made. Since the actuator acts as a low pass filter, the limitation of the proposed model is that it cannot predict accurately the response at higher frequencies greater than 1 Hz which is the pass band of the tubular actuator.

VI. CONCLUSION AND FUTURE WORK

The results show that the displacement of tubular DEA can be predicted closely by using a hybrid model that combines the physics based approach and lumped parameter modeling of the tubular actuator. The error between the predicted displacement and experimental displacement is small and hence the model may be used for dynamic analysis of the tubular DEA by generating a state space model.

Future work involves utilizing a more complex model to accurately predict displacements over large mechanical loads and strains as well as to account for the membrane stiffening. The Gent, Ogden, and Yeoh models are good candidates to use as a model that can cover large stretch regions. Since

the VHB dielectric elastomer membranes have high viscous effects, it is worth looking into models that incorporate this effect with a relaxation time that affects the dynamics of the membrane with time during loading and unloading as well as with the frequency of the membrane actuation.

REFERENCES

- [1] P. Brochu and Q. Pei, "Advances in dielectric elastomers for actuators and artificial muscles," *Macromolecular rapid communications*, vol. 31, pp. 10–36, 01 2010.
- [2] R. K. Katzschmann, J. DelPreto, R. MacCurdy, and D. Rus, "Exploration of underwater life with an acoustically controlled soft robotic fish," *Science Robotics*, vol. 3, no. 16, 2018.
- [3] A. Marchese, C. Onal, and D. Rus, "Autonomous soft robotic fish capable of escape maneuvers using fluidic elastomer actuators," *Soft Robotics*, vol. 1, pp. 75–87, 03 2014.
- [4] R. Pelrine, P. Sommer-Larsen, R. D. Kornbluh, R. Heydt, G. Kofod, Q. Pei, and P. Gravesen, "Applications of dielectric elastomer actuators," in *Smart Structures and Materials 2001: Electroactive Polymer Actuators and Devices*, Y. Bar-Cohen, Ed., vol. 4329, International Society for Optics and Photonics. SPIE, 2001, pp. 335 349.
- [5] R. Pelrine, R. D. Kornbluh, J. Eckerle, P. Jeuck, S. Oh, Q. Pei, and S. Stanford, "Dielectric elastomers: generator mode fundamentals and applications," in *Smart Structures and Materials 2001: Electroactive Polymer Actuators and Devices*, Y. Bar-Cohen, Ed., vol. 4329, International Society for Optics and Photonics. SPIE, 2001, pp. 148 – 156
- [6] G. Kovacs, P. Lochmatter, and M. Wissler, "An arm wrestling robot driven by dielectric elastomer actuators," *Smart Material Structures*, vol. 16, pp. 306–, 04 2007.
- [7] P. Chakraborti, H. K. Toprakci, P. Yang, N. D. Spignal, P. Franzon, and T. Ghosh, "A compact dielectric elastomer tubular actuator for refreshable braille displays," *Sensors and Actuators A: Physical*, vol. 179, pp. 151 157, 2012.
- [8] M. Tryson, H.-E. Kiil, and M. Benslimane, "Powerful tubular core free dielectric electro activate polymer (DEAP) push actuator," in *Electroactive Polymer Actuators and Devices (EAPAD)* 2009, Y. Bar-Cohen and T. Wallmersperger, Eds., vol. 7287, International Society for Optics and Photonics. SPIE, 2009, pp. 447 – 457. [Online]. Available: https://doi.org/10.1117/12.815740
- [9] R. Sarban, R. Jones, B. Mace, and E. Rustighi, "A tubular dielectric elastomer actuator: Fabrication, characterization and active vibration isolation," *Mechanical Systems and Signal Processing*, vol. 25, no. 8, pp. 2879 – 2891, 2011.
- [10] J.-S. Plante and S. Dubowsky, "Large-scale failure modes of dielectric elastomer actuators," *International Journal of Solids and Structures -INT J SOLIDS STRUCT*, vol. 43, 04 2006.
- [11] R. Sarban, B. Lassen, and M. Willatzen, "Dynamic electromechanical modeling of dielectric elastomer actuators with metallic electrodes," *IEEE/ASME Transactions on Mechatronics*, vol. 17, no. 5, pp. 960– 967, Oct 2012.
- [12] R. Sarban and R. W. Jones, "Physical model-based active vibration control using a dielectric elastomer actuator," *Journal of Intelligent Material Systems and Structures*, vol. 23, no. 4, pp. 473–483, 2012.
- [13] G. Rizzello, D. Naso, A. York, and S. Seelecke, "Closed loop control of dielectric elastomer actuators based on self-sensing displacement feedback," Smart Materials and Structures, vol. 25, no. 3, p. 035034, feb 2016.
- [14] Z. Suo, "Theory of dielectric elastomers," Acta Mechanica Solida Sinica, vol. 23, no. 6, pp. 549 – 578, 2010.
- [15] T. He, L. Cui, C. Chen, and Z. Suo, "Nonlinear deformation analysis of a dielectric elastomer membrane-spring system," *Smart Materials and Structures*, vol. 19, no. 8, p. 085017, 07 2010.
- [16] B. Kim, S. B. Lee, J. Lee, S. Cho, H. Park, S. Yeom, and S. Park, "A comparison among neo-hookean model, mooney-rivlin model, and ogden model for chloroprene rubber," *International Journal of Precision Engineering and Manufacturing*, vol. 13, 05 2012.
- [17] T. Lu, J. Huang, C. Jordi, G. Kovacs, R. Huang, D. R. Clarke, and Z. Suo, "Dielectric elastomer actuators under equal-biaxial forces, uniaxial forces, and uniaxial constraint of stiff fibers," *Soft Matter*, vol. 8, no. 22, pp. 6167–6173, 2012.